Int. J. Heat Mass Transfer. Vol. 13, pp. 927–931. Pergamon Press 1970. Printed in Great Britain

SHORTER COMMUNICATIONS

A CORRELATION OF LOCAL NUSSELT NUMBERS FOR LAMINAR FLOW HEAT TRANSFER IN ANNULI

RICHARD J. NUNGE, EARNEST W. PORTA and RONALD BENTLEY

Department of Chemical Engineering, Clarkson College of Technology, Potsdam, New York, U.S.A.

(*Received* 26 *May* 1969 *and in revised form* 19 *November* 1969)

NOMENCLATURE

A, dimensionless velocity gradient, $\partial\bar{u}/\partial\bar{y}$, evaluated at $\bar{y} = 0$;

c, dimensionless velocity gradient, $\partial\bar{u}/\partial y$, evaluated at $y = 0$;

h, heat-transfer coefficient defined by equation (5);

k, thermal conductivity;

Nu, Nusselt number defined by equation (4);

$Nu_{\text{W.S.}}$, $\dfrac{2(r_o - r_i)q_w}{k(T_w - T_m)}$;

Nu_{LMR}, $\dfrac{hD_e}{k} = \dfrac{\Phi_{jj}}{\theta_{jj} - \theta_{mj}}$;

Nu^*, Nusselt number defined by equation (13);

p, 0 for UWT, 1 for UWF;

q_w, heat flux at the wall;

r, radial coordinate;

$\bar{r}$, dimensionless radial coordinate, r/r_o;

r^*, radius ratio, r_1/r_o;

s, -1 for $j = o$, $+1$ for $j = i$;

T, temperature;

$\bar{T}$, dimensionless temperature, $(T - T_e)/(T_w - T_e)$ for a uniform wall temperature $(T - T_e)/(q_w r_j/k)$ for a uniform wall flux;

$\bar{T}^{(2)}$, $\dfrac{T - T_e}{q_w(r_o - r_i)/k}$;

$\bar{T}^{(3)}$, $\dfrac{T - T_e}{T_w - T_e}$;

$\bar{u}$, dimensionless velocity, u/u_m;

x, axial coordinate;

$\bar{x}$, $\alpha x/[(r_0 - r_i)^2 u_m]$.

$\bar{x}_t$, $\dfrac{4\sigma^3}{9}$;

y, dimensionless radial coordinate, $s(r - r_j)/r_j$;

$\bar{y}$, $\dfrac{s(\bar{r} - \bar{r}_j)}{(1 - r^*)}$.

Greek symbols

α, thermal diffusivity;

β, y/σ;

θ, $\bar{T}$ for a uniform wall temperature or $\bar{T}/\sigma$ for a uniform wall flux;

λ, $\dfrac{\alpha x}{u_m r_j^2 c} = \dfrac{\bar{x}}{A}\left(\dfrac{1 - r^*}{\bar{r}_j}\right)^3$;

σ, (9λ) ;

Φ, $2q_w(r_o - r_i)/(k[T_w - T_e])$;

ϕ, expansion function.

Subscripts

e, entrance;

i, inner wall;

j, heated wall;

m, mean;

o, outer wall;

w, wall;

∞, asymptotic.

HEAT transfer in annuli has been studied analytically by several investigators [1–3] using both Levêque and Graetz type approaches. The results are characteristically dependent on the radius ratio r^* and each value of the radius ratio requires a completely new solution of the energy equation. Worsøe-Schmidt [1] presented a similarity solution of the same nature as the classical Levêque solution except that it included a fully developed velocity profile and the effects of curvature, while Lundberg *et al.* [2] obtained a solution similar to the classical Graetz expansion. These yield overlapping results for intermediate axial distances. Because the Nusselt numbers obtained in these studies depend on the radius ratio, a large number of curves are required to present an extensive investigation of the variation of the Nusselt number with r^*. One of the objectives of the present study is to find a method of correlating the results for different annuli so that the numerical results can be more easily applied to design problems.

Also investigated are two of the simplifying assumptions that have been employed in many studies of heat and mass transfer systems wherein the temperature or concentration

changes are confined to a boundary layer which is thin compared to the momentum boundary layer. These assumptions are that the velocity distribution is linear and that the effect of curvature is negligible. The limitations of these assumptions employed singly or together have not been clearly established, although it is certain that they yield accurate results at small axial distances from the onset of the concentration or temperature boundary layer.

This latter objective will be considered first because it provides a basis for reaching the other objectives. Therefore, the predictions obtained in the thermal entrance region of annular passages with either a uniform wall temperature (UWT) or uniform wall flux (UWF) will be compared for three different models. These are: Case 1, curvature and fully developed velocity included; Case 2, curvature and linear approximation to the velocity; and, Case 3, the Levêque solution. Results for Case 1 are given by Worsøe-Schmidt [1] while Case 2 is developed in this paper. It should be noted that a generalized approach for deriving higher order correction terms to asymptotic results for laminar forced convection heat or mass transfer was developed by Acrivos and Goddard [4] and that the method of solution used for Cases 1 and 2 is really a specialized application of this approach.

ANALYSIS AND RESULTS FOR CASE 2

Using the linear approximation to the velocity distribution, the dimensionless energy equation in cylindrical coordinates becomes

$$y\frac{\partial \bar{T}}{\partial \lambda} = \frac{\partial^2 \bar{T}}{\partial y^2} + \frac{s}{1+sy}\frac{\partial \bar{T}}{\partial y}. \tag{1}$$

The subscript j will be used to indicate whether the thermal boundary layer is developing over the inside wall of the annular space ($j = i$, $s = 1$) or inside the outside wall ($j = o$, $s = -1$).

To solve equation (1), the similarity coordinate

$$\beta = y/\sigma \tag{2}$$

is introduced where

$$\sigma = (9\lambda)^{\frac{1}{3}}.$$

Proceeding in the usual manner [1, 5. 6] of expanding θ in a power series in σ with coefficients $\phi_n(\beta)$, an equation similar to equation (11b) of [1] is obtained for the ϕ_n with the right-hand side replaced by

$$\sum_{m=1}^{\infty} (-s)^m \beta^{m-1} \phi'_{n-m}(\beta), \quad n = 1, 2, \ldots. \tag{3}$$

The zero order coefficients, $\phi_0(\beta)$, are obtained from Case 3, the Levêque solution.

If the local Nusselt number is defined as

$$Nu_j = \frac{2hr_j}{k} \tag{4}$$

where

$$h(T_w - T_e) = -k\left.\frac{\partial T}{\partial r}\right|_{r=r_j} \tag{5}$$

then a plot of Nu_j vs. σ results in a single curve for each boundary condition at each wall. A heat-transfer coefficient based on the driving force

$$T_w - T_m$$

is used later in this paper. Since T_m is only negligibly different from T_e in the region under consideration here, the heat-transfer coefficient based on the difference between the wall temperature and the bulk mean temperature T_m will not differ significantly from that given in equation (5). The Nusselt number given by equations (4) and (5) can be expressed as

$$Nu = -2\sum_{n=0}^{\infty} \phi'_n(0)\,\sigma^{n+1}, \qquad p = 0 \tag{6}$$

$$Nu = 2/\sum_{n=0}^{\infty} \phi_n(0)\,\sigma^{n+1}, \qquad p = 1. \tag{7}$$

Quantities necessary to calculate the Nusselt numbers are given in Table 1. Note that the values of the zero order

Table 1. Expansion functions evaluated at the wall for UWF and derivatives of the expansion functions evaluated at the wall for UWT with $j = i$

n	$\phi'_n(0)$	$\phi_n(0)$
0	−1·11985	0·73488
1	−0·50047	−0·24103
2	0·070193	0·098930
3	−0·030831	−0·045047
4	0·017277	0·022072

functions for $p = 1$ and the derivatives of the zero order functions for $p = 0$ at the wall are the same for $j = o$ and i and that

$$\left.\begin{aligned} \phi'_{n_{j=o}}(0) &= (-1)^n \phi'_{n_{j=i}}(0), \qquad n > 0 \quad \text{and} \quad p = 0 \\ \phi_{n_{j=o}}(0) &= (-1)^n \phi'_{n_{j=i}}(0), \qquad n > 0 \quad \text{and} \quad p = 1 \end{aligned}\right\} \tag{8}$$

such that only one set of functions for each boundary condition need to be tabulated.

To compare the predictions of the three cases it is necessary to relate the dimensionless axial distances, $\bar{x}$, and Nusselt number definitions, $Nu_{W.S.}$, used in [1] to those used here. These are summarized below.

$$\lambda = \frac{\bar{x}}{A}\left(\frac{1-r^*}{\bar{r}_j}\right)^3, \qquad \bar{r}_j = \frac{r_j}{r_0}, \qquad r^* = \frac{r_i}{r_o} \tag{9}$$

$$Nu_j = \frac{\bar{r}_j}{1 - r^*} Nu_{\text{W.S.}_j}(1 - \bar{T}^{(3)}_{m,j}); \quad p = 0 \qquad (10)$$

$$Nu_j = \frac{\bar{r}_j}{1 - r^*}\left(\frac{\bar{T}^{(2)}_j - \bar{T}^{(2)}_{m,j}}{\bar{T}^{(2)}_j}\right) Nu_{\text{W.S.}_j}; \quad p = 1 \qquad (11)$$

$$\bar{T}^{(2)}_{m,j} = \frac{2\bar{r}_j\bar{x}}{(1 + r^*)}. \qquad (12)$$

Since the radius ratio, r^*, appears as a parameter for Case 1, functions similar to the ϕ_n's used here must be computed for each value of r^* considered. Thus the computational effort is reduced substantially by making the linear approximation to the velocity distribution.

To test the validity of the assumptions, the local Nusselt numbers obtained for Cases 2 and 3 were compared to the more exact solution. The agreement breaks down only at larger values of σ where the thermal boundary layer has grown to a significant fraction of the annular gap and one would ordinarily use a Graetz-type solution. Similar results were obtained at the outside wall.

The improvement in the Levêque solution, Case 3, brought about by including the effects of curvature for the outside wall is shown on Fig. 1. At very small values of σ the local Nusselt numbers for all three cases are the same. As σ increases however, the results for Case 2 are more nearly in agreement with Case 1. The maximum value of σ for which the Nusselt numbers for Case 2 are within 5 per cent or less of those for Case 1 is a slight function of the radius ratio and the boundary condition, the agreement being better for smaller r^* and for the UWF boundary condition. To insure 5 per cent

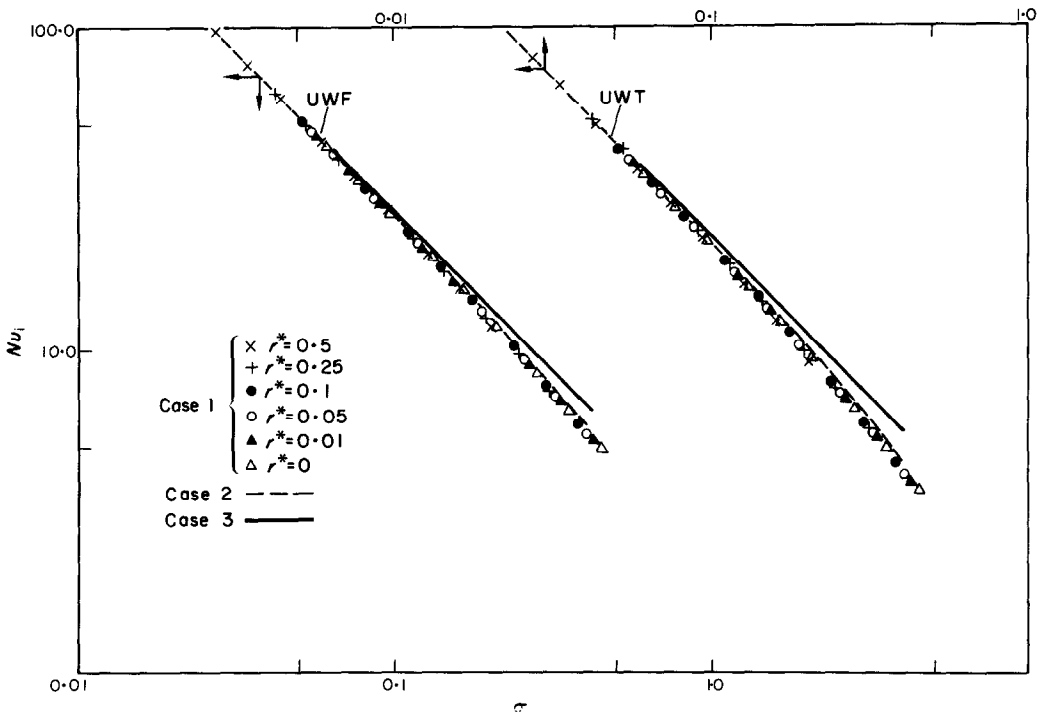

FIG. 1. A comparison of the local Nusselt numbers defined by equations (12) and (13) for Cases 1, 2 and 3 with $j = o$.

more exact solution given by Case 1 and the result at the inside wall is shown in Fig. 1. Nusselt numbers defined by equations (4) and (5) were computed for Case 1 using the results tabulated in [1] and are shown on Fig. 1 for various radius ratios. The results for Cases 2 and 3 are shown as dashed and solid lines respectively. This figure illustrates clearly that the Nusselt numbers for all radius ratios are well correlated by a single curve for any given boundary condition and that the results for Case 2 are in good agreement with the accuracy for the UWT boundary condition in Case 2 requires $\sigma \leqslant 0{\cdot}1$ for $r^* = 0{\cdot}5$ and $\sigma \leqslant 0{\cdot}2$ for $r^* \leqslant 0{\cdot}25$. For Case 3, $\sigma \leqslant 0{\cdot}06$ is required for all r^*. At $\sigma = 0{\cdot}1$ the Levêque solution is 5 per cent higher than Case 2. For 5 per cent accuracy with the UWF in Case 2 the limits are $\sigma \leqslant 0{\cdot}15$ for $r^* = 0{\cdot}5$ and $\sigma \leqslant 0{\cdot}25$ for $r^* \leqslant 0{\cdot}25$. For the Levêque solution $\sigma \leqslant 0{\cdot}1$ is needed.

A comparison for the three cases at the inside wall shows that the results for Case 1 are bracketed by the other two

with the Levêque solution below and the linear approximation above the exact solution. The Levêque solution is slightly better than Case 2 with $r^* \geqslant 0.5$ and a UWT boundary condition since $\sigma \leqslant 0.3$ yields 5 per cent accuracy in Case 3 while $\sigma \leqslant 0.175$ is required for Case 2. For $r^* \leqslant 0.25$ the limits are 0.2 and 0.4 for Cases 3 and 2 respectively. For the UWF condition Case 2 requires $\sigma \leqslant 0.25$ for $r^* = 0.5$ while for $r^* \leqslant 0.25$ the results are still within 5 per cent or less of those for Case 1 up to $\sigma = 0.1$. Case 3 requires $\sigma \leqslant 0.3$ for $r^* = 0.5$ and $\sigma \leqslant 0.175$ for $r^* \leqslant 0.25$.

The results for the three cases were also compared on the basis of the definitions given in [1]. This is essentially a comparison of the dimensionless wall fluxes and mean temperatures for UWT and the dimensionless wall temperature for UWF. In general Case 2 predicts values which are higher than those for Case 1 for UWT while for UWF, Case 2 predicts a lower wall temperature and a larger Nusselt number. At the outside wall, the errors associated with Case 2 are magnified in Case 3 and Case 2 gives a more accurate result for the radius ratios considered here ($r^* \leqslant 0.5$). For example at $\bar{x} \times 10^{-3}$, with $r^* = 0.02$, $j = o$ and $p = 0$, the values of Φ and T_m for the three cases are 12.934, 13.20, 14.203 and 0.03930, 0.03982, 0.04177 respectively. At the inside wall the results for Case 1 lie between those for Cases 2 and 3. For small radius ratios, Case 2 is more accurate; for example, with $p = 1$, $r^* = 0.1$ and $\bar{x} = 10^{-4}$, the wall fluxes for Cases 1, 2 and 3 are 60.873, 62.75 and 54.153 respectively. More complete comparisons are available elsewhere [7].

CORRELATION EXTENDED TO LARGER AXIAL DISTANCES

The preceding comparisons have shown that the radius ratio can be eliminated as a parameter and that when it is eliminated, accurate values of the local Nusselt number can be obtained in the thermal entrance region. In order to determine if r^* can be eliminated for larger axial distances the results of Lundberg *et al.* (LMR), modified by the geometry correction suggested by equations (10) and (11), were plotted against the new axial corrdinate, σ.

The Nusselt number used by LMR is defined in terms of the equivalent diameter and the bulk mean temperature. This was converted to Nusselt number based on the radius of the heated wall by using equation (13)

$$Nu_j^* = Nu_{\mathrm{LMR}}\left(\frac{\bar{r}_j}{1-r^*}\right) = \frac{\Phi_{jj}}{\theta_{jj}-\theta_{mj}}\frac{\bar{r}_j}{1-r^*} \qquad (13)$$

and plotted vs. σ for several different cases. Typical examples are shown in Figs. 2 and 3 (more complete tabluated comparisons are available in [7]). The Worsøe-Schmidt results are also included on these figures. From these figures it is clear that correlating the local Nusselt numbers in this manner causes the curves for different values of the radius ratio to fall on a single curve over almost the entire range of interest. Deviations occur only as the asymptotic region is approached.

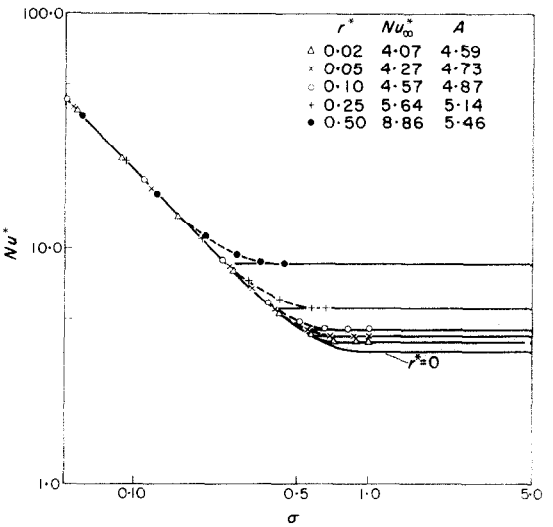

FIG. 2. The local Nusselt number for the fundamental solution of the 2nd kind defined by equation (22) for r^* with $j = o$.

The new correlation together with an expression for the asymptotic Nusselt number provides a rapid estimation of the local Nusselt number over the entire range of σ.

The curved solid line through the results for the outside wall heated on Fig. 2 represents the limiting case of $r^* = 0$, the circular tube obtained from the results of Brown [8] for $\bar{x}_i \geqslant 0.04$. For smaller values of $\bar{x}_i$ the tabulated results of Worsøe-Schmidt for $r^* = 0$ were used. Sparrow *et al.* [9] give the tube results for UWF.

A comparison between the results predicted by the modified tube solution used in conjunction with $Nu^*_{\infty j}$ and the LMR and WS results for several values of r^* shows excellent agreement for all but a small region where the local Nusselt number is approaching the asymptotic value. The maximum error here is approximately 10 per cent and this may be reduced by joining the asymptotic line and the tube solution with a smooth transition line.

When the inner wall is being heated the tube solution no longer represents a limiting case since as r^* goes to 0, the inner wall disappears. In this case the solution for the smallest r^* studied in the literature, $r^* = 0.02$ was used to form the lower portion of the limiting curve near the asymptotic region in Fig. 3. An expression for the upper portion of the limiting curve was obtained using the solution of W-S for $r^* = 0.10$, the smallest value of r^* for which a solution is given. For uniformity it would have been desirable to use the same r^* in the development of the limiting solution in both regions, but it is not necessary. The only requirement is that the two solutions overlap since all results fall on a single curve. A comparison of the results predicted by the limiting solution and the Nusselt numbers of LMR and W-S for

several values of r^* shows the same type of agreement as in the previous case.

The results presented here and elsewhere provide the basis for a rapid estimation of the local Nusselt number for any r^* at any axial location. For example, if A is computed from

$$A = \frac{2s(1-r^*)}{\bar{r}_j[1+r^{*2}-(1-r^{*2})/(-\ln r^*)]} \times \left[\frac{(1-r^{*2})}{(-\ln r^*)} - 2\bar{r}_j^2\right] \quad (14)$$

σ can be obtained and the local Nusselt number read from a figure similar to Fig. 2 or 3 for the appropriate boundary condition.

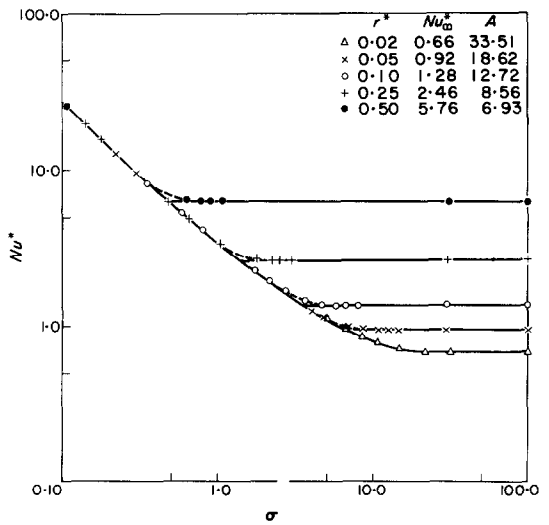

FIG. 3. The local Nusselt number for the fundamental solutions of the 3rd kind defined by equation (22) for several values of r^* with $j = i$.

Although this work has dealt only with the correlation of local Nusselt numbers, in many cases it is possible to use the same procedures in correlating mean Nusselt numbers defined as

$$Nu_m = \frac{\int_0^x Nu_{\text{Local}}(x)\,dx}{x}. \quad (15)$$

Since the mean Nusselt number is based on the local Nusselt number, it follows that an expression for the mean Nusselt number in a tube such as Hausen's [10] for UWT could be modified and used as the limiting curve for the mean Nusselt number in annuli along with a result valid for the upper portion of the limiting curve which could be developed from the solution of W-S for $r^* = 0$. Another possibility for obtaining limiting curve for the mean Nusselt number at short distances is the empirical relationship given by Sieder–Tate [11] which is valid for small mean temperature changes.

CONCLUSIONS

The limitations of the assumptions common to Levêque-type problems have been investigated. It is clear that removing each of the assumptions raises the computation time substantially. The improvement brought about by including the effects of curvature over the Levêque solution is important at larger values of the axial distance. As expected, the effects of curvature are most important for smaller radius ratios. The Nusselt numbers obtained by including both the fully developed velocity distribution and the effects of curvature in the energy equation correlate well over significant axial distances with the solution in which r^* is not a parameter, thus indicating the usefulness of the linear approximation to the velocity distribution.

When the Nusselt number is defined in terms of r_j as in equation (13) instead of the equivalent diameter; the radius ratio is effectively eliminated as a parameter. This can be seen in Figs. 2 and 3, where the curves for all values of r^* form a single curve and deviate from it only as the asymptotic value of the Nusselt number is approached.

ACKNOWLEDGEMENTS

Ronald Bentley was a participant in the Undergraduate Participation Program sponsored by the National Science Foundation during the course of this work. Support of the OSW is also acknowledged.

REFERENCES

1. P. M. WORSØE-SCHMIDT, *Int. J. Heat Mass Transfer* **10**, 541 (1967).
2. R. E. LUNDBERG, W. C. REYNOLDS and M. W. KAYS, NASA Technical Note D-1972 August 1963.
3. M. JAKOB and K. A. REES, *Trans. Am. Inst. Chem. Engrs* **37**, 619 (1941).
4. A. ACRIVOS and J. D. GODDARD, *J. Fluid Mech.* **23**, Part 1, 273 (1965).
5. A. M. MERCER, *Appl. Scient. Res.* **A9**, 450 (1960).
6. W. N. GILL, D. W. ZEH and CHI TIEN, *A.I.Ch.E. Jl* **12**, 1141 (1966).
7. E. W. PORTA, Ph.D. Dissertation, Clarkson College, in progress (1969).
8. G. M. BROWN, *A.I.Ch.E. Jl* **6**, 179 (1961).
9. E. M. SPARROW, A. HALLMAN and R. SIEGEL, *Appl. Scient. Res.* **A7**, 386 (1960).
10. J. G. KNUDSEN and D. L. KATZ, *Fluid Dynamics and Heat Transfer*, p. 371. McGraw Hill, New York (1958).
11. E. N. SIEDER and G. E. TATE, *Ind. Engng Chem.* **28**, 1429 (1936).